Carpathian Journal of Earth and Environmental Sciences, February 2021, Vol. 16, No. 1, p. 199 – 210; DOI:10.26471/cjees/2021/016/167

HIGH RESOLUTION MINERALOGICAL CHARACTERIZATION OF SEDIMENTS - LAKE BOLĂTĂU-FEREDEU (ROMANIA)

Máté KARLIK[1,2,4], Ildikó GYOLLAI[2], Anna VANCSIK[3,5], Krisztián FINTOR[4], Zoltán SZALAI[3,5], Marcel MÎNDRESCU[6], Ionela GRĂDINARU[6], Sándor VÁGÁSI[7], Gábor BOZSÓ[4], Márta POLGÁRI[2,8] & Elemér PÁL-MOLNÁR[4]

[1]Isotope Climatology and Environmental Research Centre, Institute for Nuclear Research, H-4026 Bem tér 18/c Debrecen, Hungary, karlikmate@gmail.com

[2]Institute for Geological and Geochemical Research, Research Centre for Astronomy and Earth Sciences, ELKH, Budapest. Hungary

[3]Geographical Institute, Research Centre for Astronomy and Earth Sciences, Budapest, Hungary

[4]Department of Mineralogy, Geochemistry and Petrology, University of Szeged, Szeged, Hungary

[5]Department of Environmental and Landscape Geography, Eötvös Loránd University, Budapest, Hungary

[6]Department of Geography, Ştefan cel Mare University, Suceava, Romania

[7]Copenhagen, Denmark

[8]Eszterházy Károly University, Dept. of Natural Geography and Geoinformatics, Eger, Hungary

Abstract: The catchment (bedrock and soil) and sediments of lake Bolătău, Romania were studied by high resolution multi-methodological investigations to characterize paleoenvironmental and formation conditions. Particle size analyses, optical and cathodoluminescence microscopy, FTIR-ATR and Raman spectroscopy, X-ray powder diffraction, and XRF were applied for microtextural, chemical, micro-mineralogical and embedded organic material characterization and distribution of the sediments, especially concerning geochemical conditions, like pH and redox potential change. Our results support physical and chemical weathering in the process of soil formation with appearance of the new minerals appear (10Å sized phyllosilicates and clay minerals). Comparison of these studies offer possible differentiation of syn- and diagenetic mineralization, the clarification of debris contribution, microbial mediation and complex mineralization via decomposition of cell and extracellular polymeric substance. Based on the analyses on the abrasives, a suboxic environment prevailed in the depositional area and considerable microbial contribution is proposed via accumulation of lake sediments.

Key words: lake sediment, high resolution analysis, mineralized biosignatures, biomineralization

1. INTRODUCTION

The lake sediments are one of the most common popular study field in the paleoenvironmental topic because lakes are excellent indicators of environmental change (Battarbee, 2000). In the last fifty years, numerous studies have been performed on the methodology of paleolimnological research (Kummel & Raup, 1965; Berglund, 1986; Last & Smol, 2001). A number of approaches are used in this multidisciplinary field. Regarding the research topic, a number of organic and inorganic components were used in the paleoenvironmental research (e.g. Meyers & Teranes, 2002; Grygar et al., 2006; Eglinton & Eglinton, 2008; Bordon et al., 2009; Buczkó et al., 2009; Gąsiorowski & Sienkiewicz, 2010). The Romanian Carpathians have many lakes suitable for this type of research and, also, deserves special attention. In the past period several papers have been elaborated using organic and inorganic proxies (e.g. Magyari et al., 2009, Tóth et al., 2018). Detailed knowledge of the catchment was essential for the success of these researches.

To understand the process of sediments formation a detailed knowledge of the catchment area is required. The rock layer is the main starting material for inorganic components. The milling process is influenced by a number of parameters and knowledge

of these processes facilitates subsequent analyzes (Wan et al., 2019). If more than one chemical composition is found in the catchment area, the direction of each element can be taken into account in the subsequent analysis of the sediment, for example in the event of precipitation events or changes in cover. Chemical and biological processes in the soil result in changes in the composition of the existing or new minerals. Vegetation from microbial levels to trees has a prominent role in such processes (Jackson et al., 1948; Sverdrup, 2009). The formation and composition of lake sediments depend on a number of parameters that greatly influence the results of subsequent organic and inorganic geochemical analyzes. Preliminary microscopic microtextural observations raised considerable microbial contribution to the sediment. Based on this, the aim of the study was the high resolution microtextural, micro-mineralogical and embedded organic material characterization and distribution of the sediment, especially concerning geochemical conditions, like pH and redox potential change. These studies offer possible differentiation of syn- and diagenetic mineralization, the clarification of debris contribution, microbial mediation and complex mineralization via decomposition of cell and extracellular polymeric substance (EPS) (Polgári et al., 2019).

2. GEOLOGICAL BACKGROUND, CATCHMENT AREA, SAMPLING

2.1. Geological background

The study area was located in the East-Carpathian region near to the catchment of Sadova river, Romania. The geology of region where the locality is placed belongs to the westernmost sub-unit (Black Shales Formation) of the Audia Nappe (Fig. 1), comprising, mostly Cretaceous shales (Săndulescu, 1984). The catchment of the lake Bolătău is the eastern part of the mentioned region. This small area consists of three different geological formations. The Cretaceous deposits are predominantly clayey, and the Palaeogene ones are mostly represented by uniform layers of sandstone, with small intercalations of clays and marly clays. The study catchments are situated within the westernmost sub-unit (Black Shales Formation) of the Audia Nappe comprising shales of Cretaceous age. These geological formations are highly susceptible to landsliding as they comprise alternations of black marly shales, glauconitic, siliceous or calcareous sandstones, red, green, striped, and grey clays (Fig. 1) (Ionesi, 1971; Mîndrescu et al., 2013).

2.2. Location and main details of the lake Bolătău and the catchment area

Sadova stream is a tributary of river Moldova - Romania. The Bolătău lake (47° 37′ 20.74″ N, 25° 25′ 54.43″ E) means pond of puddle, which is a common name in the region (Grădinaru et al., 2012). The lake is near to Feredeului Mts., just below the Obcina Feredeului peak (1364 m asl) and in the neighborhood to the Lezer lake. A landslide event indicated the catchment and the lake current formation (Mîndrescu et al., 2013).

The lake maximum depth was 5.2 m and the surface 0.3 ha in 2010. The water quality was measured in 2010, the total phosphorus concentration in the lake was 0.014 mg/L (Mîndrescu et al., 2010), corresponding to mesotrophic class regarding the trophic status (OECD, 1982). The dissolved oxygen measurements were made in 2014. It was measured at four profiles. In the top of the lake the dissolved oxygen value was between 8-9 mg/L, which attenuate to 0.2 mg/L in the deepest section. Indeed, these redox conditions make the bottom water to become very methanogenic (Karlik et al., 2018).

The landslide, expanding over ca. 30 ha, affected mainly the right-side slope, as well as the valley head slope to a lesser extent (Mîndrescu et al., 2010). The catchment diameter is only 700 m but the elevation amplitude within the catchment is significant, amounting to ca. 227 m (1364 m a.s.l. to 1137 m a.s.l.) (Mîndrescu et al., 2013). The flora of the catchment is currently composite. 6 ha of the catchment is deforested and variants of herbs can be found. Currently the main species of the conifer forest (24 ha) are Norway spruce (Picea abies) and silver fir (Abies alba), goat's willow (Salix caprea), alder (Alnus incana), trembling aspen (Populus tremula), birch (Betula pendula) that can be found at the lake shore, and among water-loving herbaceous plants the rush (Bolbosschoenus sp.) occurs (Mîndrescu et al., 2010).

2.3. Sampling

The catchment area is small but the relief dates are varied. To correctly analyze the catchment material and identify the starting material in the sediments for comparison, the catchment soil and the bedrock were sampled during 2016 to 2020 years period. Sampling was performed at random in areas demarcated on the basis of environmental variations. The random samples from each territory were homogenized. After homogenization/mixture, three representative rock samples and three soil samples were compound.

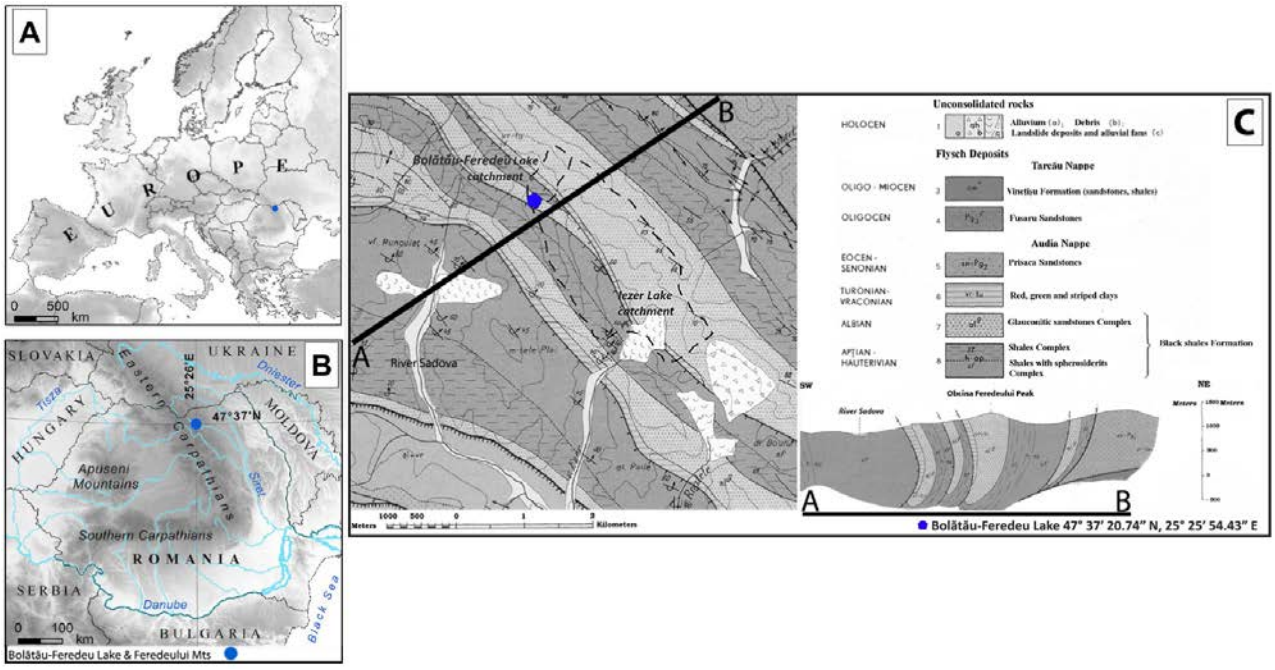

Figure 1. Location of Lake Bolătău-Feredeu A) at continental scale; B) in the Eastern Carpathian region, national scale; C) closer view of the research area (Pojorâta geological map, 1:50 000 scale - Geological Institute of Romania

In the catchment area three different regions of the bedrock and soil were located: “up side”; “right side” and “left side”. The soil samples were collected near to the bedrock deposits. Bulk samples of lake sediment, catchment soil samples (~5 sample/area) and homogenised to 1 sample/area, and bedrock samples from 3 area (~5-7 sample/area) and homogenized to 1 sample/area (bulk measurement) were analysed by XRD and XRF.

Lake sediments were analyzed with especially sonar. The reflection from the different sediment layers help to decide the most promising drilling points in the center of the lake. The sediment cores were collected during to April of 2013. At that time the lake surface was frozen. The sediments were drilled with two different type of corer instruments (Russian corer and a gravity corer).

Due to the corers parameter which was similar (the d=6.5 +/-0.1 cm and the S= 33.2 ± 0,6 cm^2), the sampling points were very close, (distance between the two sampling points is less than 1 m). The collected cores have between 66 cm and 400 cm length. The cores and the layers wet condition was documented, descripted and photographed. The overlapping region of the two cores fitted perfectly based on comparison of characteristic zones of the cores (Mîndrescu et al., 2016).

2.4. Chronology of the sediment

In the multi proxy analyses one of the most important things is the correct dating and the perfect

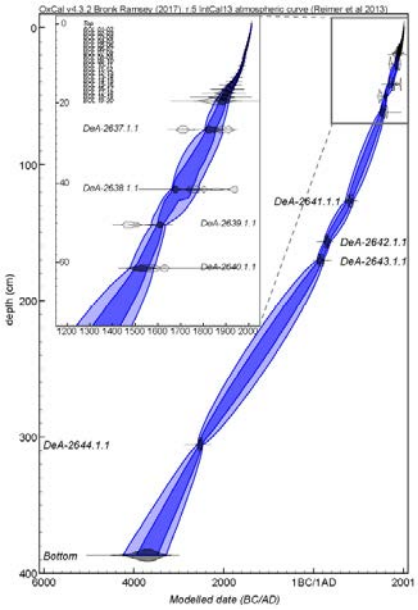

Figure. 2 Sediment chronology of the Bolătău-Feredeu sequence. Light (dark) shading shows the 95% (68%) confidence range of the Bayesian model. Original and modelled probability density functions of the radiometric ages are plotted by light and dark grey, respectively. Uppermost 70 cm is enlarged offering a more detailed image (Karlik et al., 2018)

time model events or changes (Birks & Birks, 2006). The first detailed micro sedimentological and geochronological analyses proved the great potential of the Bolătău sediment archive for future high resolution paleolimnological investigations (Mîndrescu et al., 2016). To make a high-quality time model the sediment chronology model was based on

two different isotopes methods: the chronology based on radiocarbon (Mîndrescu et al., 2016) and the another one, Pb-210 ages (Bihari et al., 2018).

Pb-210 (T1/2=22.23 yr) is one of the most used isotopes in the first 150 years sediment dating processes and used in lakes with similar conditions in Romania (Appleby, 2001 & 2008; Begy et al., 2009 & 2011). The Pb-210 chronology and the calculations were published in Bihari et al., (2018), where they used different accumulation models in the calculated Pbex-210 (Fig. 2).

Each model and measurement were validated with two Cs-137 fallout events (nuclear weapon test 1963 & Chernobyl NPP accident 1986). The final chronology was based on Pb-210 ages for the top 20 cm and 8 AMS ^{14}C ages. The model built with P_Sequence function of the Oxcal v.4.2 (Bronk Ramsey, 2009) program. The same software was used for the calibration of ^{14}C dates to calendar years in conjunction with the Northern Hemisphere IntCal13 (Reimer et al., 2013) dataset. The bottom of the lake sediments was ~6000 year old (Karlik et al., 2018).

3. METHODS

In this study, bulk samples were investigated from the past 600 years. List of samples and the used methods are summarized in Table 1.

Table 1: List of samples and the used methods

Sample ID	Desc-ription	Methods					
		OM	CL	FTIR	Ram	XRD	XRF
6	microbialite	49		79	20		
8	microbialite	37 (24)	24	23	20		
10	microbialite	45 (32)	32	20	20		
15	microbialite	46		17	20		
Lake sediment bulk samples						63	63
Catchment soil (~5 sample/area) and homogenised to 1 sample/area						3	3
Bedrock sample from 3 area (~5-7 sample/area) and homogenized to 1 sample/area (bulk measurement)						3	3
Total		177	56	139	80	69	69

Abbrev.: OM: optical rock microscopy; CL: cathodoluminescence microscopy; Ram: Raman spectroscopy; FTIR: infrared spectroscopy, XRD: X-ray powder diffraction, XRF: X-ray fluorescence spectroscopy.

Particle size distribution was determined by Fritsch Analysette 22 Microtech Plus laser diffraction particle size analyzer, which measures in the range of 0.08 μm - 2.0 mm. Samples were treated for carbonate and organic matter removal according to USDA (United States Department of Agriculture) NRCS method (Burt, 2004). Three particles/pieces (ca. 1 g) were taken from each treated sample. Five minutes of ultrasonic treatment and sodium-pyrophosphate (55 g l-1) was applied to allow a complete dispersion of the specimens. Refractive index and the imaginary part were assumed to be 1.54 and 0.01 (Eshel et al., 2004; Varga et al., 2015). The percentage of sand (2000–50 μm), silt (50–2 μm) and clay fractions (below 8 μm) were reported, according to a modified USDA texture classification scheme (Konert & Vandenberghe, 1997).

The mineral components were measured by Rigaku Miniflex600 power diffractometer. It has got a theta/2theta configuration with graphite monochromator. Instrument build in Rh-tube with Cu anode (used X-ray line is Cu KA1&KA2 (1,54060 KeV & 154443 KeV). Under the measurement process generator setting was 50Kv/10mA and the goniometer speed was 2°/min with 0,5° step size. Diffractograms were measured by 2 to 70 degree. Sample preparation procedure: The representative samples were powered in agate mortal, then the main composite was measured with oriented sample preparation. The XRD system detection limit is ~5 V/V%.

The chemical composition of lake sediment samples were measured with RIGAKU Supermini wavelength dispersive X-Ray fluorescence spectrometer with Pd X-ray tube 50 kV excitation voltage and 40 anodes current. EZScan was the applied measuring method the time of measurements from Fluorine to uranium was 40 minutes. The catchment bedrock and the sediment samples were analyzed in Spectro xSort XRF & Docking station system. The used fundamental parameter calibration: Mining - FP (Mg to Uranium). The measurement time with two filter was 180 sec. The EZ-Scan and the Mining calibration reliability was tested with international lake sediment standards.

Petrographic structural-textural studies were made on ten representative thin sections taken from different depths in transmitted light by optical rock microscopy (NIKON SMZ800 microscope and NIKON ECLIPSE 600 rock microscope). 177 photos of representative sections were taken.

Cathodoluminescence (CL) petrography was carried out on 2 thin sections using a Reliotron cold cathode cathodoluminescence apparatus mounted on a BX-43 Olympus polarization microscope. Accelerating voltage was 7-7.7 keV during the analysis. Cathodoluminescence spectra were recorded by using an Ocean Optics USB2000+VIS-NIR spectrometer. Spectrometer specifications are 350-1000 nm wavelength range, and 1.5 nm (FWHM)

optical resolution. For characterization of CL 56 photos were taken.

High resolution *in situ* micro-Raman spectroscopy was used for micro-mineralogy and organic matter identification and distribution. Raman spectra acquired along lines vertical to observed lamination of samples, where the distance between each point was 10 µm. A Thermo Scientific DXR Raman Microscope was used with a 532 nm (green) diode pumped solid-state (DPSS) Nd-YAG laser using 3 mW laser power, 50x objective lens in confocal mode (confocal aperture 25 µm pinhole). Full acquisition time/measuring point was 1 min (acquisition time: 3 sec; number of exposures: 20 sec) and spectral resolution was ~2 cm^{-1} at each measurement. Diagrams were organized on peak height versus analytical spot number of each of the phases along the Raman scanned section (80 spectra were acquired). Intensities were normalized to the highest peak for each spectrum. The following Raman bands were used for normalization: anatase: ~144 cm^{-1}; quartz: ~463 cm^{-1}; K-feldspar: ~513 cm^{-1}. Identification of minerals was made with the RRUFF Database (Database of Raman – spectroscopy, X-ray diffraction, and chemistry of minerals: http://rruff.info/). Contamination by epoxy glue was taken into consideration.

Fourier transform infrared spectrometer (FTIR) was used for in situ micro-mineralogy and organic material identification on five thin sections (139 spectra), using a Bruker FTIR VERTEX 70 equipped with a Bruker HYPERION 2000 microscope with a 20x ATR objective and MCT-A detector. During attenuated total reflectance Fourier transform infrared spectroscopy (ATR) analysis, the samples were contacted with a Ge crystal (0.5 micron) tip with 1 N pressure. The measurement was conducted for 32 seconds in the 600–4000 cm^{-1} range with 4 cm^{-1} resolution. Opus 5.5 software was used to evaluate the data. Contamination by epoxy glue, glass, wood stick, and dichloromethane were taken into consideration.

4. RESULTS

High resolution microtextural, particle size analyses and also *in situ* mineralogical and organic matter determination and distribution were made.

4.1. Particle size analyses, mineralogy and chemistry

The values of the particle size analyses were distributed to four sections, colloid fraction <0.5 µm, clay fraction <8 µm, silt fraction from 8 µm to 50µm, and sand fraction from 50 µm to 2000 µm.

All of the soil samples gave similar result, the clay fraction was between 45 to 60 %, the silt fraction was between 38 to 47 %. The sand fraction was less than 10%. In the lake sediment samples colloid fraction have been the less fraction in this measurement, the maximum value was 2 % and the minimum 0.9 %. The average of the colloid fraction was 1.5 % with scatter of 0.4 %. The clay and silt fractions were the most dominant fractions in the lake sediment samples. The average of the clay fraction was 43.2 % with 5.4 % scatter and the silt fraction was 52.4%, with 5.2 % scatter. The dominant particle size of the material vary from 0.5 - 8 µm to 50 µm. The sand fraction was only 4 % with 2.2 % scatter. The classification was elaborated based on Konert & Vandenberghe's (1997) (Fig. 3). Most of the samples are located (placed) in the silty-clay class, 9 samples were in silty clay loam and only one in the full clay class. No sand fraction occurred.

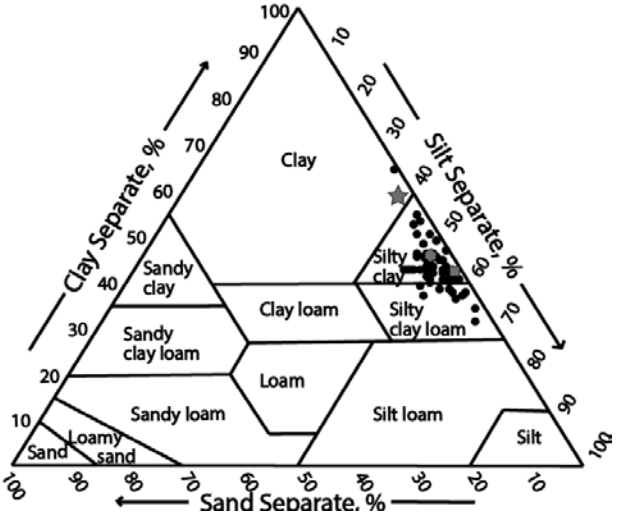

Figure 3. Sediment classification based on Konert & Vandenberghe (1997). (Black – lake sediment; star – right side soil; circle – left side soil; square – upper side soil

The bedrock is mixture of sandstone and shales complex. The XRD analyses of the three bedrock samples showed the same composition (quartz).

Soil samples were richer in minerals, same to the bedrock samples, the left and up side samples are also, the same, the two samples include: quartz, 10Å phyllosilicate, and clay minerals (near to the detection limit). The right side soil sample includes: quartz, 10Å phyllosilicate, plagioclase, chlorite, illite or smectite, and kaolinite. Mineral composition of the lake sediment is: quartz, 10Å phyllosilicate, plagioclase, clay minerals, and magnetite/maghemite. The lake sediment doesn't include carbonates by XRD measurements.

In the catchment three different regions of the bedrock and soil were located: "up side"; "right side" and "left side". The element composition of the collected bedrock in the up side and left side was

similar to each other the SiO_2 concentration is higher than ~90 % and the Al_2O_3 concentration is near ~2.8%. The chemical composition of the bedrock of the third area was strongly different, the SiO_2 concentration was ~70%, and the second dominant element fraction was the Al_2O_3 with ~16%. The soil samples were collected near from the bedrock deposits. The measured samples were richer in elements than the bedrock samples. The soil samples of the three area represent the same element composition. The first 65 cm represent time period between AD. 1400 - A.D. 2000. The 63 particles element composition data has been averaged to help the comparison with the bedrock and the soil data. (Table 2) Figure 4 shows the position of samples in weathering diagram, which help to understand the origin of the sediments. The calculation is based on Kronberg & Nesbitt (1981). The sodium content was under the detection limit in all samples.

4.2. Optical rock microscopy

Optical microscopy in the thin sections (samples 6, 8, 10 and 15) represent variable microtextural features of mineralized microbialite. Panorama photos show fine lamination (Fig. 5). Brown, woven, organic matter-rich structures represent series of biomat-like and stromatolitic structures, which are common (mineralized biosignatures of microbial activity and mineralized biosignatures of putative Fe-oxidizing bacteria (FeOB). Rarely larger well-structured microfossils also occurred (Fig. 5). In very high resolution (100-1000x) the whole samples were densely woven by filamentous inner necklace-like microstructures or coccoid forms, aggregates and vermiform brain-like micro-textures (mineralized biosignatures). These filaments contain randomly disseminated 0.5-1 µm large mineral phases (Fig. 5).

CL photos showed very fine grained randomly disseminated particles, which showed scarce bright yellow luminescence (apatite) and dull blue luminescence (quartz). Along microbialite laminae segregated quartz occurred (Fig. 5).

The Raman spectroscopy measurements determined carbonaceous matter (CM) with low maturity, which occur at each measuring point along both sections. However, enrichment of CM related to lamination of the samples were not observable along the sections. Most probably quartz, feldspar and anatase grains occur in the sample.

FTIR-ATR analyses were carried on four thin sections selected on observation by optical microscopy. Mineral composition is feldspar, apatite, quartz, montmorillonite, ferrihydrite and chlorite. Highly variable embedded organic matter occurred in all samples (C=N/CH-amid, graphite, O=C, dCH2, C-O). Details of two representative samples are presented in the tables (Table 3 and 4).

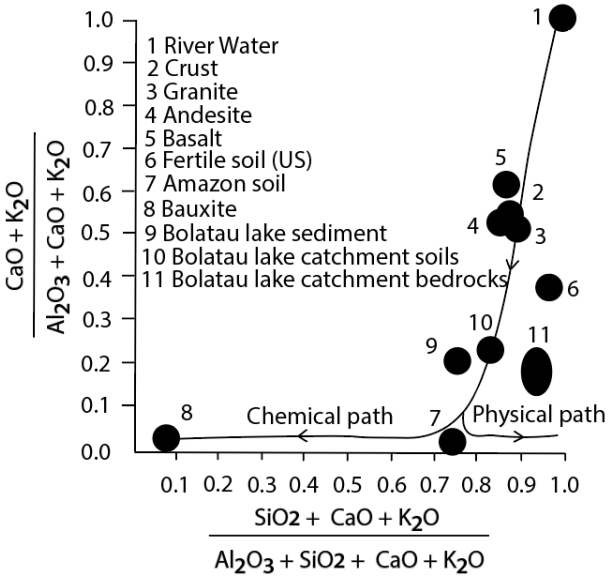

Figure 4. Theoretical weathering curves of the Bolătău bedrock, soil, and lake samples (based on Kronberg & Nesbitt, 1981)

Table 2: Element composition data (1: Bedrock up side; 2: Bedrock left side; 3: Bedrock right side; 4: Soil up side 5:

	MgO %	Al_2O_3 %	SiO_2 %	SO_3 ppm	K_2O %	CaO %	TiO_2 %	Fe_2O_3 %	Zn ppm	Rb ppm	Sr ppm	Y ppm	Zr ppm
1	<0.5	2.6	91.51	53	0.7	0.1	0.3	4.1	34	19	22	9	117
2	<0.5	3.0	94.	<46	1.3	0.1	0.3	3.0	50	39	37	8	116
3	0.9	16.3	70.9	564	2.5	0.2	0.8	5.3	104	90	69	22	246
4	<0.8	18.0	76.9	167	2.6	0.2	0.6	4.6	93	101	60	13	139
5	<0.5	14.4	62.6	983	3.2	1.0	0.9	3.0	62	133	92	10	146
6	<0.7	15.6	57.5	<51	3.8	0,05	0.9	7.2	94	178	75	14	146
7	0.4	1,7	49,5	5275	3.3	0.9	0.8	5.2	183	222	101	nd	nd
8	16	13	3	34	6	8	10	9	14	12	15	nd	nd

Soil left side; 6: Soil right side; 7: Lake sediment average; 8: Lake sediment relative deviation, nd: no data

Table 3. FTIR dataset of sample No. 6

No. 6		**Measuring area**										
Wavelength (cm^{-1})	Type Wavelength (cm^{-1})	1 n: 5*	2 n: 6	3 n: 9	4 n: 7	5 n: 10	6 n: 8	7 n: 4	8 n: 6	9 n: 15	10 n: 9	Ref.
Organic matter												
1170	v C-O	x	x	x	x	x	x	x	x	x	x	1
1360-1450	vs CO	x	x	x	x	x	x	x	x	x	x	1
1454-1482	d CH2	x	x	x	x	x	x	x	x	x	x	1
1526	C-N, CH deformation	x	x	x	x	x	x	x	x	x	x	1
1540-1550	C-N N-H amide II		x									1
1598	C=C asym. Stretch		x			x	x	x			x	1
1632-1652	amide I C=O, C-N, N_H											1
1720-29	v as COOH											1
1799	C-O											1
2343	CO	x	x	x	x	x	x	x	x	x		2
2365	CO	x	x	x	x	x	x	x	x	x		2
2853	C-H sym. Stretch CH2									x		1
2926	C-H asym. Stretch CH2									x		1
Mineralogy												
feldspar	798, 950, 1000	x	x	x	x	x	x	x	x	x	x	2
quartz	685, 773, 808, 1055, 1083			x	x					x	x	2
apatite	790, 1012, 1093		x								x	3
montmorillonite	988, 779, 1000, 1615, 3600							x				4
ferrihydrite	Fe-O, 692, 830, 930		x								x	5

Legend: * n: number of acquired spectra; References: 1: Parikh & Chorover (2006), 2: Müller et al. (2014), 3: Beasley et al. (2014), 4: Madejová & Komádel (2001), 5: Glotch & Rossmann (2009)

Table 4. FTIR dataset of sample No. 10

No. 10		**Measuring area**				
Wavelength (cm^{-1})	**Type Wavelength (cm^{-1})**	**1 n: 5***	**2 n: 6**	**3 n: 5**	**4 n: 4**	**Ref.**
Organic matter						
1170	v C-O	x	x	x	x	1
1360-1450	vs CO	x	x	x	x	1
1454-1482	d CH2	x	x	x	x	1
1526	C-N, CH deformation	x	x	x	x	1
1540-1550	C-N N-H amide II		x			1
1598	C=C asym. Stretch	x	x			1
1632-1652	amide I C=O, C-N, N_H					1
1720-29	v as COOH					1
1799	C-O					1
2343	CO	x			x	2
2365	CO	x			x	2
2853	C-H sym. Stretch CH2					1
2926	C-H asym. Stretch CH2					1
Mineralogy						
feldspar	798, 950, 1000	x	x	x	x	2
apatite	790, 1012, 1093					3
montmorillonite	988, 779, 1000, 1615, 3600					4
chlorite	980, 3400				x	6
ferrihydrite	Fe-O, 692, 830, 930					5

Legend: * n: number of acquired spectra; References: 1: Parikh & Chorover (2006), 2: Müller et al. (2014), 3: Beasley et al. (2014), 4: Madejová & Komádel (2001), 5: Glotch & Rossmann (2009), 6: Udvardi et al. (2014)

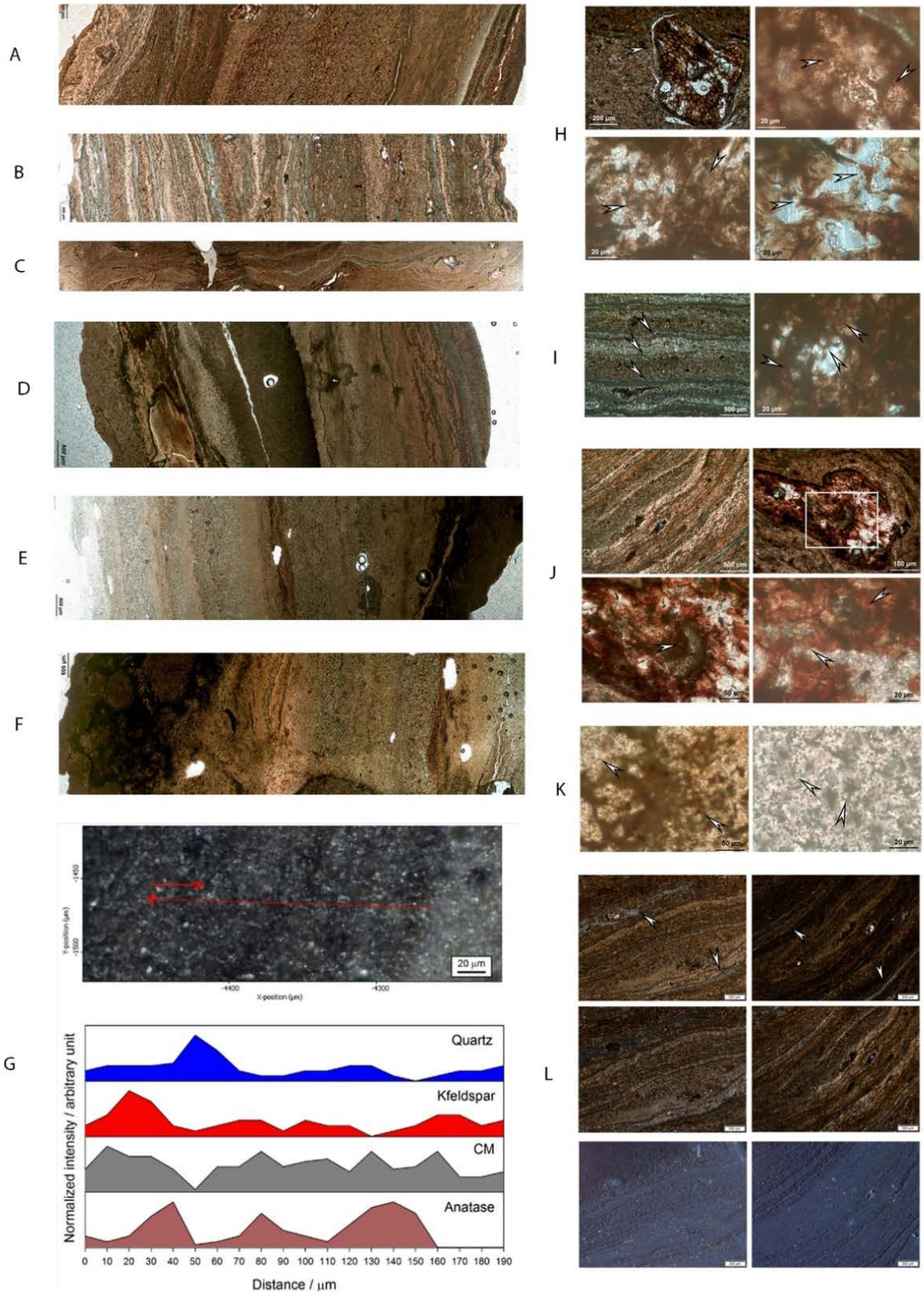

Figure 5. Panorama figures of thin section profiles (optical rock microscopy, transmitted light, 1N, photo composition (A: Section 6; B: Section 8; C: Section 10; D: Section 15A; E: Section:15B; F: Section 15B); High resolution in situ micro-Raman spectroscopy (G); Mineralized microbialite microtextural features (H: Section 6; I: Section 8; J: Section 10; K: Section 15); Cathodoluminescence microscopy (L) Arrows show segregated quartz. On the CL images very small minerals show cathodoluminescence: bright yellow-apatite, blue-quartz

5. DISCUSSION

Source area of these sediments is in direct connection with the geological unit where Bolătău lake is placed. The bedrock XRF and XRD analyses confirm the findings has sense of the find the objects of Ionesi (1971) and Mîndrescu et al. (2013) concerning mineralogy and chemistry.

In the catchment area two, a little bit different bedrocks are located, one is mostly sandstone (samples from the upside and left side) with high SiO_2 content (more than 90%). The mineralogy of the second bedrock type is also sandstone with clay mineral content (samples from the right side) and it has got a high aluminum content in addition to silicon (SiO_2:~70% Al_2O_3:~16%) - Table 2. Because the catchment area is closed by mountains, this material has been the primary source of the soil and lake sediment in the last 6000 years. The bedrock surface is transformed to soil material by physical weathering.

The chemical parameters give us information on the weathering processes. Compared with the bedrock chemical composition, two types of weathering processes were realized (Fig. 4). Physical and chemical weathering resulted the final form of the soil. The sand size faction was less than 10%, in the future studies this information can be used to understanding the environmental signals in the sediment (precipitation events, or high impact energy effects, deforestation, etc.). The right side area soil classification was “Clay” type, another two area soils were “Silty clay” type. In the classification diagram right side soil sample position was near to the border line of “Silty clay”. The mineral composition of soils is same: quartz, 10Å phyllosilicate and clay minerals, and in the right side sample extra further mineral, plagioclase occur. Based on dataset of the soil samples around the lake, it is not necessary to take into account the possible preferred directions of leaching when examining the lake sediment.

The two most dominant lake sediment particle sizes were clay and silt fraction (43.2 ±5.4% and 52.4 ±5.2%). The sand fraction is only 4 ±2%. The significant changes are the result of high intensity environmental changes. The Loss-on-Ignition ( ) value is around 20% in each sample, because the sediment is carbonate free it come from the organic material. The SO_3 component had the biggest changes with 34%. The SO_2 signal significantly come from the organic material. The organic material refers to paleoenvironmental information about the catchment (Karlik el at., 2018), namely the change of n-alkanes refers to deforestation event.

Optical rock microscopy (1N and xN) transmitted light photos do not support debris contribution on considerable level.

XRD mineralogy and Raman spectroscopy determined quartz, 10Å phyllosilicate, plagioclase, clay minerals, magnetite/maghemite as main constituents, and also apatite, and feldspar. These fit with the FTIR results, but FTIR is more sensitive. FTIR identified variable organic matter as main constituent, and mineral assemblage of apatite, feldspar, poorly crystallized segregated quartz (wide peaks), rarely ferrihydrite and montmorillonite. The size of minerals is very small, 0.5-1 μm, which disseminate in the network of the organic matter in the extracellular polymeric substance (here after EPS). Size distribution study also resulted 30-40% of grains below 8 μm. These grains do not follow the lamination of microbialite and their small size, and also their CL features (no luminescence) support complex early diagenetic mineralization based on microbial mediation and cell and EPS decomposition rather than debris material contribution. It is also supported by the mineral assemblage (apatite, feldspar, poorly crystallized segregated quartz (wide peaks), rarely ferrihydrite and montmorillonite) which is typical for these processes. Based on these results this basin is a starving one in sense of debris contribution. Details on complex mineralization on the pool of microbially mediated elements fit well with the results of Polgári et al. (2019). Concerning the formation conditions of minerals support suboxic, slightly alkaline conditions, which turned locally to anoxic, represented by pyrite formation.

6. CONCLUSION

The bedrock measurements confirm the findings of Ionesi (1971) and Mîndrescu et al. (2013) concerning mineralogy and chemistry. But the chemical differences between the bedrock types element composition much higher than the expectation. The mineral composition in the two average sample were similar: quartz, and one is different: quartz and clay minerals. It was confirmed by the chemical analysis. The sandstone was fragmented during physical weathering to the soil primary material.

Physical and chemical weathering in the soil took place in parallel. The weathering processes were modified by the chemical and mineral composition. The chemical and mineral composition of the soil samples is not highly different. Some new minerals were detected by XRD: quartz, 10Å phyllosilicate, plagioclase, chlorite, illite or smectite, and kaolinite. The differences observed in the bedrock samples, do not appear predominantly in the soil samples.

Sediment size classification based on Konert & Vandenberghe (1997) were “Clay” and “Silty clay”.

The most dominant size of lake sediment fractions were clay and silt. Their distribution changed with depth. The chemical composition ranged over a wide interval. It was likely that the inorganic parameters of the lake sediment provide an opportunity for paleoenvironmental reconstruction. The interpretation of the data may be aided by previous organic geochemical results included in Karlik et al (2018). Based on the analyses on the abrasives, a suboxic environment prevailed in the sediment and considerable microbial contribution is proposed via accumulation of lake sediment.

Acknowledgement

The authors thank for the support by the National Research, Development and Innovation Office, Hungary, National Scientific Research Fund No. 125060. The authors thank for the support by the European Union and the State of Hungary, co-financed by the European Regional Development Fund in the project of GINOP-2.3.2.-15-2016-00009 ‘ICER’.

REFERENCES

Appleby, P.G., 2001. *Chronostratigraphic techniques in recent sediments.* In: In: Last, W.M., Smol, J.P. (Eds.), Tracking Environmental Change Using Lake Sediments, vol. 1. Springer, Netherlands, pp. 171–203. http://dx.doi.org/10.1007/0-306-47669-X_9.

Appleby, P.G., 2008. *Three decades of dating recent sediments by fallout radionuclides, a review.* Holocene 18 (1), 83–93. http://dx.doi.org/10.1177/0959683607085598.

Battarbee, R.W., 2000. *Palaeolimnological approaches to climate change, with special regard to the biological record.* Quaternary science reviews 19(1), 107-124. https://doi.org/10.1016/S0277-3791(99)00057-8

Beasley, M.M., Bartelink, E.J., Taylor, L. & Miller, R.M., 2014. *Comparison of transmission FTIR, ATR, and DRIFT spectra: implications for assessment of bone bioapatite diagenesis.* Journal of Archaeological Science, 46, pp.16-22.

Begy, R., Cosma, C. & Timar, A., 2009. *Recent changes in Red Lake (Romania) sedimentation rate determined from depth profiles of 210Pb and 137Cs radioisotopes.* J. Environ. Radioact. 100 (8), 644–648. http://dx.doi.org/10.1016/j.jenvrad.2009.05.005.

Begy, R., Timar-Gabor, A., Somlai, J. & Cosma, C., 2011. *A sedimentation study of St. Ana Lake (Romania) applying the 210Pb and 137Cs dating methods*. Geochronometria 38 (2), 93–100. http://dx.doi.org/10.2478/s13386-011-0017-6.

Berglund, B. E. (ed.), 1986. *Handbook of Holocene Palaeoecology and Palaeohydrology*. John Wiley & Sons, New York, 869 pp.

Bihari, A., Karlik, M., Mindrescu, M., Szalai, Z., Grădinaru, I., & Kern, Z. 2018. Fallout isotope chronology of the near-surface sediment record of Lake Bolătău. *Journal of environmental radioactivity*, *181*, 32-41.

Birks, H.H. & Birks, J.H.B., 2006. *Multi-proxy studies in palaeolimnology*. Veg. Hist. Archaeobotany 15, 235–251.

Bordon, A., Peyron, O., Lézine, A.M., Brewer, S., Fouache, E., 2009. *Pollen-inferred late-glacial and Holocene climate in southern Balkans (Lake Maliq).* Quaternary International 200(1), 19-30. https://doi.org/10.1016/j.quaint.2008.05.014

Bronk Ramsey, C., 2009. *Bayesian analysis of radiocarbon dates.* Radiocarbon 51 (1), 337–360. https://doi.org/10.1017/S0033822200033865.

Buczkó, K., Magyari, E.K., Bitušík, P. & Wacnik, A., 2009. *Review of dated Late Quaternary palaeolimnological records in the Carpathian Region, east-central Europe.* Hydrobiologia, 631(1), 3-28. http://dx.doi.org/10.1007/s10750-009-9800-2

Burt R. (Ed.) 2004. *Soil Survey Laboratory Methods Manual. Soil Survey Investigations Report No. 42*. USDA Natural Resources Conservation Service. Washington, D. C.

Eglinton, T.I., Eglinton, G., 2008. *Molecular proxies for paleoclimatology*, Earth and Planetary Science Letter 275, 1-16 https://doi.org/10.1016/j.epsl.2008.07.012.**Eshel, G., Levy, G.J., Mingelgrin, U. & Singer M. J.,** 2004. *Critical Evaluation of the Use of Laser Diffraction for Particle-Size Distribution Analysis.* Soil Science Society of America Journal. 68, 736–743

Eshel, G., Levy, G.J., Mingelgrin, U. & Singer M. J., 2004. *Critical Evaluation of the Use of Laser Diffraction for Particle-Size Distribution Analysis.* Soil Science Society of America Journal. 68, 736–743.

Gąsiorowski, M., Sienkiewicz, E., 2010. *20th century acidification and warming as recorded in two alpine lakes in the Tatra Mountains (South Poland, Europe).* Science of the Total Environment 408(5), 1091-1101. https://doi.org/10.1016/j.scitotenv.2009.10.017

Glotch, T.D. & Rossman, G.R.., 2009: *Mid-infrared reflectance spectra and optical constants of six iron oxide/oxyhydroxide phases.* Icarus 204 663–671.

Grădinaru, I., Iosep, I., Pociask-Karteczka, J., Brancelj, A. & Mácha, P., 2012. *Study of the occurrence and distribution of „Iezer“ and „Bolătău“- based toponyms in Romania and their counterparts from Poland, the Czech Republic and Slovenia.* Georeview 21, 68–79.

Grygar, T., Kadlec, J., Pruner, P., Swann, G., Bezdička, P., Hradil, D., Lang K., Novotna K., & Oberhänsli, H. 2006. *Paleoenvironmental record in Lake Baikal sediments: environmental changes in the last 160 ky.* Palaeogeography, Palaeoclimatology, Palaeoecology, 237(2-4), 240-254.

Ionesi, L. (Ed.), 1971. *Flişul Paleogen Din Bazinul Văii*

Moldovei. Academiei, Bucureşti.

Jackson, M. L., Tyler, S. A., Willis, A. L., Bourbeau, G. A., & Pennington, R. P., 1948. *Weathering sequence of clay-size minerals in soils and sediments. I. Fundamental generalizations.* The Journal of Physical Chemistry, 52(7), 1237-1260.

Karlik, M., Fekete, J., Mîndrescu, M., Grădinaru, I., Bozsó, G., Bíró, L., & Kern, Z., 2018. *Natural and anthropogenic changes in a lake-forest system in Bukovina (Romania) since 1340 AD documented by sedimentary organic geochemistry (C, N and n-alkanes).* Quaternary International, 493, 166-175.

Konert, M. & Vandenberghe, J., 1997. *Comparison of laser grain size analysis with pipette and sieve analysis: a solution for the underestimation of the clay fraction.* Sedimentology. 44, 523–535.

Kronberg, B. I., & Nesbitt, H. W., 1981**.** *Quantification of weathering, soil geochemistry and soil fertility.* Journal of Soil Science, 32(3), 453-459.

Kummel, B. & D. Raup (eds.), 1965. *Handbook of Paleontological Techniques.* W. H. Freeman and Company, San Francisco, 862 pp.

Last W. M. & Smol J. P. (eds.), 2001. *Tracking Environmental Change Using Lake Sediments. Volume 2: Physical and Geochemical Methods.* Kluwer Academic Publishers, Dordrecht, The Netherlands

Madejová, J. & Komadel, P., 2001. *Baseline studies of the clay minerals society source clays: infrared methods.* - Clays and Clay Minerals, 49, 410-432.

Magyari, E.K., Braun, M., Buczkó, K., Kern, Z., László, P., Hubay, K. & Bálint, M. 2009. Radiocarbon chronology of glacial lake sediments in the Retezat Mts (South Carpathians, Romania): a window to Lateglacial and Holocene climatic and paleoenvironmental changes. Central European Geology 52: 225-248. DOI:10.1556/CEuGeol.52.2009.3-4.2

Magyari, E.K., Veres, D., Wennrich, V., Wagner, B., Braun, M., Jakab, G., Karátson, D., Pál, Z., Ferenczy, Gy., St Onge, G, Rethemeyer, J., Francois, J.P., Reumond, F., Schäbitz, F., 2014. Vegetation and environmental responses toclimate forcing during the Last Glacial Maximum and deglaciation in the East Carpathians: attenuated response to maximum cooling and increased biomass burning. Quaternary Science Reviews 106, 278-298. https://doi.org/10.1016/j.quascirev.2014.09.015

Meyers P.A. & Teranes J.L., 2002 *Sediment Organic Matter*. In: Last W.M., Smol J.P. (eds) Tracking Environmental Change Using Lake Sediments. Developments in Paleoenvironmental Research, vol 2. Springer, Dordrecht

Mîndrescu, M., Cristea, A.I. & Florescu, G., 2010. *Water quality and ecology of the Iezer and Bolătău lakes.* Romanian J. Limnol. Lakes, Reservoirs Ponds 4, 117–130.

Mîndrescu, M., Cristea, A.I., Hutchinson, S.M., Florescu, G. & Feurdean, A., 2013. *Interdisciplinary investigations of the first reported laminated lacustrine sediments in Romania.* Quaternary International 239, 219–230. http://dx.doi.org/10.1016/j.quaint.2012.08.2105.

Mîndrescu M., Németh A. Grădinaru I., Bihari Á., Németh T., Fekete J., Bozsó G. & Kern Z., 2016 *Bolătău sediment record – Chronology, microsedimentology and potential for a high resolution multimillennial paleoenvironmental proxy archive. Quaternary* Geochronology Volume 32, 11-22.

Müller, C. M., Pejcic, B., Esteban, L., Delle Piane, C., Raven, M., & Mizaikoff, B., 2014. *Infrared Attenuated Total Reflectance Spectroscopy: An Innovative Strategy for Analyzing Mineral Components in Energy Relevant Systems.*Scientific reports, 4.

OECD, 1982. *Eutrophication of Waters, Monitoring. Assessment and Control*, Paris.

Parikh, S. J., & Chorover, J., 2006. *ATR-FTIR spectroscopy reveals bond formation during bacterial adhesion to iron oxide.* Langmuir, 22(20), 8492-8500.

Reimer, P.J., Bard, E., Bayliss, A., Beck, J.W., Blackwell, P.G., Bronk Ramsey, C., Grootes, P.M., Guilderson, T.P., Haflidason, H., Hajdas, I., Hatte, C., Heaton, T.J., Hoffmann, D.L., Hogg, A.G., Hughen, K.A., Kaiser, K.F., Kromer, B., Manning, S.W., Niu, M., Reimer, R.W., Richards, D.A., Scott, E.M., Southon, J.R., Staff, R.A., Turney, C.S.M. & Plicht, J., 2013. *IntCal13 and Marine13 radiocarbon age calibration curves 0-50,000years cal BP*. Radiocarbon 55 (4), 1869–1887. https://doi.org/10.2458/azu_js_rc.55.16947.

Polgári, M., Gyollai, I., Fintor, K., Horváth, H., Pál-Molnár, E., & Biondi, J. C. 2019. Microbially mediated ore-forming processes and cell mineralization. *Frontiers in Microbiology*, *10*, 2731.

Săndulescu, M., 1984. *Geotectonica României. Editura Tehnica*, Bucureşti.

Sverdrup, H., 2009. *Chemical weathering of soil minerals and the role of biological processes.* Fungal Biology Reviews. 23. 94-100. 10.1016/j.fbr.2009.12.001.

Tóth, M., Buczkó, K., Specziár, A., Heiri, O., Braun, M., Hubay, K., Czakó, D. & Magyari. E.K., 2018. *Limnological changes in South Carpathian glacier-formed lakes (Retezat Mountains, Romania) during the Late Glacial and the Holocene: A synthesis.* Quaternary International, 477: 138-152 https://doi.org/10.1016/j.quaint.2017.05.023

Udvardi, B., Kovács, I. J., Kónya, P., Földvári, M., Füri, J., Budai, F., **& Mihály, J**., 2014. Application of attenuated total reflectance Fourier transform infrared spectroscopy in the mineralogical study of a landslide area, Hungary. Sedimentary Geology, 313, 1-14.

Varga, Gy., Újvári, G., Kovács, J. & Szalai, Z., 2015. *Effects of particle optical properties on grain size measurements of aeolian dust deposits.* Geophysical Research Abstracts. vol. 17, EGU 2015-9848-1.

Wan, J., Tokunaga, T.K., Williams, K.H., Dong, W. Brown, A., Henderson., N., Newman., A.W., Hubbard, S.S., 2019. *Predicting sedimentary bedrock subsurface weathering fronts and weathering rates.* Scientific Report 9, 17198 https://doi.org/10.1038/s41598-019-53205-2

Received at: 27. 11. 2020
Revised at: 12. 02. 2021
Accepted for publication at: 16. 02. 2021
Published online at: 18. 02. 2021